RESEARCH

Cell contractility and focal adhesion kinase control circumferential arterial stiffness

Emilia Roberts, Tina Xu and **Richard K Assoian**

Department of Systems Pharmacology and Translational Therapeutics, Institute for Translational Medicine and Therapeutics, University of Pennsylvania, Philadelphia, Pennsylvania, USA

Correspondence should be addressed to R K Assoian: assoian@pennmedicine.upenn.edu

Abstract

Arterial stiffening is a hallmark of aging and cardiovascular disease. While it is well established that vascular smooth muscle cells (SMCs) contribute to arterial stiffness by synthesizing and remodeling the arterial extracellular matrix, the direct contributions of SMC contractility and mechanosensors to arterial stiffness, and particularly the arterial response to pressure, remain less well understood despite being a long-standing question of biomedical importance. Here, we have examined this issue by combining the use of pressure myography of intact carotid arteries, pharmacologic inhibition of contractility, and genetic deletion of SMC focal adhesion kinase (FAK). Biaxial inflation-extension tests performed at physiological pressures showed that acute inhibition of cell contractility with blebbistatin or EGTA altered vessel geometry and preferentially reduced circumferential, as opposed to axial, arterial stiffness in wild-type mice. Similarly, genetic deletion of SMC FAK, which attenuated arterial contraction to KCl, reduced vessel wall thickness and circumferential arterial stiffness in response to pressure while having minimal effect on axial mechanics. Moreover, these effects of FAK deletion were lost by treating arteries with blebbistatin or by inhibiting myosin light-chain kinase. The expression of arterial fibrillar collagens, the integrity of arterial elastin, or markers of SMC differentiation were not affected by the deletion of SMC FAK. Our results connect cell contractility and SMC FAK to the regulation of arterial wall thickness and directionally specific arterial stiffening.

Introduction

The arterial system is composed of large, elastic arteries such as the aorta and carotids and smaller muscular arteries (1, 2, 3, 4). The large arteries undergo periodic cycles of contraction and relaxation, which help to dampen changes in arterial pressure during the cardiac cycle. These arteries contain a thin layer of endothelial cells called the 'intima' that provides a non-thrombogenic surface around the lumen, a thick 'media' comprised of vascular smooth muscle cells (SMCs) that mediate periodic arterial contraction, and a relatively diffuse outer layer called the 'adventitia' that contains fibroblasts as well

as inflammatory and precursor cells. Large arteries also contain an extensive extracellular matrix (ECM), and the two best-studied arterial ECM components, elastin and fibrillar collagens, have important and distinguishable roles in arterial mechanics. Elastin allows for arterial recoil and dominates arterial stiffness at low stress and stretch, while arterial collagens (mostly collagen-I) drive arterial stiffness in response to higher stress and stretch.

Arterial stiffening with aging and vascular disease has often been viewed as a consequence of ECM remodeling (typically, increased abundance of fibrillar collagens and/

or degradation of elastin (2, 3)). However, arterial stiffness is better conceptualized as the combined contributions of 'material' and 'functional' (also called 'structural') stiffness (3, 5). Material stiffness is thought to reflect the contribution of the arterial ECM, while functional stiffness incorporates vessel geometry (diameter, wall thickness, etc.) as well as material stiffness (3, 5).

Arterial stiffness can be studied *in vivo* by pulse wave velocity, but this approach tends to provide less mechanical insight than can be obtained by *ex vivo* methods. Pulling on isolated aortic rings or indenting on the luminal surface of isolated arterial (e.g. with an atomic force microscope) have been mainstay approaches. However, these procedures are performed in the absence of arterial pressure. This limitation can be addressed by performing inflation-extension tests on a pressure myograph, which not only measures the arterial response to physiological or pathological pressures but can also distinguish directionally specific arterial stiffening (5, 6). Using this approach, we and others have shown that age-dependent stiffening occurs in both the axial and circumferential directions (7, 8, 9, 10).

Recent work with the large arteries of genetically altered mice suggests that these bi-directional changes in arterial mechanics may be differentially regulated. For example, we reported that deletion of matrix metalloproteinase-12 (MMP12) preferentially reduces axial stiffening (7), while expression of progerin (a mutant LaminA causative for Hutchinson–Guilford Progeria Syndrome) increases the abundance of medial lysyl oxidase and preferentially affects circumferential stiffening, at least early in disease progression (8). Deletion of fibulin-5 alters axial stretch (11). Each of these proteins (MMP12, lysyl oxidase, and fibulin-5) has an established role in elastin or collagen biology, supporting the important role of the ECM in arterial stiffness.

Medial SMCs (and adventitial fibroblasts) synthesize the ECM components and ECM-modifying enzymes that play an important role in arterial stiffness. However, the degree to which SMCs make and secrete ECM components is thought to depend on their differentiation state (12, 13, 14). Healthy vascular SMCs exist in a differentiated state often called 'contractile'. These cells are relatively quiescent and express high levels of smooth muscle contractile proteins (also called differentiation genes or differentiation markers) such as smooth muscle-myosin heavy chain (SM-SMC) and smooth muscle actin (SMA). The expression of SMC differentiation genes is canonically regulated by the SRF/MRTF pathway, which in turn is downstream of Rho and its effector Rho kinase (15, 16). At sites of injury or inflammation, contractile vascular SMCs can de-differentiate into a state often called 'synthetic'. A popular current model is that arterial stiffening is a consequence of SMC de-differentiation to a synthetic phenotype because de-differentiated SMCs have a reduced expression of contractile proteins and an increased ability to synthesize ECM components and ECM remodeling enzymes. Indeed, de-differentiated SMCs appear at sites of injury and inflammation coincident with arterial stiffening *in vivo* (17, 18, 19).

Several investigators have postulated that, in addition to the ECM, the intrinsic contractility of vascular SMCs themselves also contributes to large artery stiffness, particularly in aging and hypertension (20, 21, 22, 23). For example, using atomic force microscopy, others have reported that the SMCs isolated from spontaneously hypertensive rats are stiffer than SMCs isolated from normotensive controls and that this difference is dependent on actin polymerization and the Rho-Rho kinase-myosin light chain kinase (MLCK) contractility pathway (21, 23, 24, 25). Other work has uniaxially stretched artificial arteries generated with SMCs from hypertensive or aged animals. These fabricated 'arteries' were stiffer than those containing control SMCs, and this difference was again dependent on actin polymerization and contractility (21, 23). Morgan and colleagues, using uniaxial stretch of mouse aortic segments, reported that tissue stiffness is increased in response to alpha 1-adrenergic receptor activation: in young mice, this stiffening is sensitive to pharmacologic inhibition of MLCK, non-muscle myosin-II, focal adhesion kinase (FAK), and Src (20, 26, 27). Direct inhibition of myosin motors with blebbistatin reduced the Src-dependent phosphorylation of FAK and paxillin (27). However, Humphrey and colleagues have reported that medial and especially adventitial collagen levels can increase in chronic hypertensive and non-hypertensive mouse models showing a reduced arterial contractile capacity (28, 29).

While the results outlined above have implicated SMC contractility in arterial stiffness, they have relied on mechanical analyses of isolated SMCs or *ex vivo* approaches that are performed independent of biologically relevant pressure. Here, we have studied the role of cell contractility in carotid artery stiffness by combining biaxial inflation-extension tests on a pressure myograph with rapid pharmacologic inhibition of myosin motors or MLCK, calcium chelation, and genetic deletion of FAK from SMCs. Since FAK deletion is a chronic approach, we also looked for the effects of FAK deletion on the arterial ECM and SMC differentiation. Our results support and extend prior

studies supporting a direct role for SMC contractility in large artery stiffness. Additionally, they reveal that SMC FAK contributes to the contractility effect independent of changes in fibrillar collagens or SMC differentiation and that both cell contractility and SMC FAK selectively target circumferential arterial mechanics by regulating vessel geometry.

Materials and methods

Mice and artery isolation

Floxed *Ptk2* (hereafter called FAK) mice were obtained from the Mutant Mouse Repository and Research Center (MMRRC, stock number 009967-UCD), backcrossed to the C57BL/6J background for at least ten generations, and mated to a tamoxifen-inducible smooth muscle-specific Cre line ((30) also backcrossed to C57BL/6J). These mice (hereafter called FAK^ff;iCre mice) were treated with ethanol (vehicle) or tamoxifen (Sigma Aldrich) for 5 days as described (31, 32), allowed to recover for 1–2 weeks, and analyzed at 15–21 weeks of age. Male wild-type (WT) mice (C57BL/6J) were purchased from Jackson Laboratories and analyzed at 13–15 weeks of age. Mice were fed a chow diet *ad libitum*. Mice were sacrificed with CO_2. The right carotid artery was stripped of most fat *in vivo*, removed, and then briefly stored in Hanks buffered salt solution (HBSS) with magnesium and calcium without phenol red (Corning Life Sciences) prior to myography. The mice were then perfused with PBS through the left ventricle, and the left carotid artery was removed and fixed in Prefer for paraffin-embedding and tissue immunostaining. Because the Cre transgene is integrated into the Y chromosome (30), all experiments were performed on male mice. Animal protocols were approved by the University of Pennsylvania Institutional Animal Care and Use Committee.

Carotid artery immunostaining and histologic analysis

The immunofluorescence analysis of isolated carotid arteries for ECM proteins and differentiation markers was performed largely as described (8, 33) and used the following antibodies: collagen-I (Southern Biotech, birmingham, AL, USA; 1310-01; 1:300 dilution), collagen-III (Proteintech, 22734-1-AP; 1:300 dilution), collagen-V (Abcam, ab7046; 1:250 dilution), SM-MHC (Proteintech, Rosemont, IL, USA; 21404-1-AP, 1:200 dilution) or SMA (FITC-conjugated; Sigma F3777, 1:300 dilution). FAK levels were determined using a primary FAK antibody (BD

Biosciences; 610088) diluted 50-fold in 1% goat serum in PBS and then incubated for 2 h at 37°C followed by overnight incubation at room temperature. The secondary antibody for FAK (Alexa Fluor 594 goat anti-mouse IgG; Invitrogen) was used at a 100-fold dilution in 1% goat serum in PBS and incubated with the samples for 2 h at room temperature. All samples were mounted with Dapi Fluoromount-G (Southern Biotech). Results were visualized with a Nikon Eclipse 80i microscope with a QI-Click Qimaging camera. Carotid arteries were imaged at 20× magnification.

Images were quantified using Fiji. The media of each section was traced using the polygon drawing tool, and its raw integrated intensity was divided by the area of the outlined media to obtain relative fluorescence intensity. In some experiments, this procedure was repeated for the adventitial layer.

Analysis of arterial mechanics by pressure myography

Passive arterial mechanics

Axial and circumferential mechanics were determined using a DMT 114P pressure myography with force transducer largely as described (7). Right carotid arteries were isolated from male C57BL/6J mice or male FAK^ff;iCre mice, cleaned, secured to 380 μm (outer diameter) cannulas using silk sutures, and submerged in 5 mL of calcium-containing HBSS. This closed system was checked for leaks by pressurizing the vessel to 30 mm Hg using HBSS. The arteries were also visualized by light microscopy, and any remaining fat that could affect imaging was removed. The unloaded/unpressurized axial length was measured when the artery transitioned from being bent to straight, stretched to 1.7 of that length, and pressurized to 100 mm Hg for 15 min in calcium-containing HBSS. The arteries were preconditioned by cyclic pressurization three times from 0 to 140 mm Hg in 1-min intervals. Unloaded (unstretched and unpressurized) vessel wall thickness and outer diameter were measured in multiple sections after preconditioning and averaged for post-test data analysis (Supplementary Table 1, see section on supplementary materials given at the end of this article).

In vivo stretch (IVS) was determined using force-length tests largely as described (5, 7) except that the carotid arteries were axially stretched at four constant pressures (80, 100, 120, 140 mm Hg). Equilibrium force was recorded for each stretch and pressure, and the intersection of force-stretch curves defined the IVS. Loaded inner radius and wall thickness were determined from pressure-outer diameter tests with samples at their IVS and pressurized in 10-mm

Hg (30-s) steps from 0 to 140 mm Hg before returning the artery to 0 mm Hg. We confirmed the validity of our IVS determinations by measuring axial force through the circumferential tests, and we excluded samples where axial force with pressure varied from the mean by >25%.

Raw measurements of the intraluminal pressure, force transducer readings, and video-tracked outer diameter were converted into stress-stretch curves using equations 1–4.

$$\text{Axial stretch } \lambda_z = \frac{l}{L} \tag{1}$$

$$\text{Axial stress } \sigma_z = \frac{Pa^2\pi + f_T}{\pi h(2a + h)} \tag{2}$$

$$\text{Circumferential stretch } \lambda_\theta = \frac{a + h/2}{A + H/2} \tag{3}$$

$$\text{Circumferential stress } \sigma_\theta = \frac{Pa}{h} \tag{4}$$

where l and L = loaded and unloaded vessel lengths, respectively (μm), a and A = loaded and unloaded inner radii, respectively (μm), h and H = loaded and unloaded vessel wall thickness, respectively (μm), P = intraluminal pressure (mm Hg), and f_T = axial force (nN).

Vessel wall thickness was calculated in the post-test analysis based on the sample being incompressible (see (7)). Each axial and circumferential test was performed once; results were accrued from multiple mice and plotted as mean ± s.d.

Effects of FAK, blebbistatin, EGTA, and ML7 on passive mechanics

Isolated carotid arteries from WT male mice or the male FAK^ff;iCre mice treated with ethanol or tamoxifen were cleaned of excess fat, mounted on the DMT 114P pressure myograph, and incubated in 5 mL HBSS as described above. To examine the effect of blebbistatin (EMD Millipore), EGTA, and ML7 (Cayman Chemical) on passive arterial mechanics, each carotid artery of the WT and FAK^ff;iCre mice that had been subjected to passive testing was immediately de-pressurized, brought to 100 mm Hg, and then treated with the relevant reagent (10 μM blebbistatin or 2 mM EGTA for WT mice; 10 μM blebbistatin or 20 μM ML7 for FAK-deficient mice) by replacing the HBSS bath with 5 mL of reagent-containing HBSS. The complete set of axial and circumferential tests was repeated after maximum vessel dilation had occurred in response to each

reagent (5–10 min). The effect of each drug was monitored by the increase in outer diameter (in right carotid arteries at 100 mm Hg). Mean ± s.d. changes were 2.4% ± 1.7 (blebbistatin), 2.7% ± 1.8 (ML7), and 10.1% ± 3.2 (EGTA).

Statistical analysis

Statistical analyses were performed using Prism software (Graphpad). Differences in carotid artery immunofluorescence staining were analyzed using two-tailed Mann–Whitney tests. For the myography experiments, differences in IVS were analyzed by two-tailed *t*-tests. The significance of changes in the pressure-outer diameter curves, stress-stretch curves, pressure-inner radius curves, and pressure-wall thickness curves was assessed using two-way ANOVAs. The statistical tests used are identified in the respective figure legends; significance is indicated by *($P < 0.05$), **($P < 0.01$), ***($P < 0.001$), and ****($P < 0.0001$).

Results

Acute pharmacologic inhibition of carotid artery contraction selectively reduces circumferential arterial stiffness in WT mice

We began our studies on the role of cell contractility in arterial stiffness by acutely treating freshly isolated carotid arteries from WT mice with blebbistatin (a well-established inhibitor of myosin-II-mediated contractility) and then determining the consequence for arterial geometry and stiffness. Treatment times were very short (~5 min), eliminating the likelihood of long-term changes in cell differentiation or ECM composition that could confound the analysis.

Arterial mechanics were analyzed with biaxial inflation-extension tests performed at biologically relevant pressures. Each carotid artery was analyzed twice, first in the absence and then in the presence of blebbistatin. We could hardly detect an effect of blebbistatin on axial mechanics as determined by the IVS (Fig. 1A) or the axial stress–stretch relationship (Fig. 1B and Supplementary Fig. 1A, B, C). However, we detected clear effects of blebbistatin on the circumferential arterial response to increasing pressure. In particular, arterial outer diameters (Fig. 1C) and inner radius measurements (Fig. 1D) were increased in the blebbistatin-treated arteries as compared to the WT controls. The blebbistatin-treated arteries also had a significantly reduced wall thickness (Fig. 1E) in response
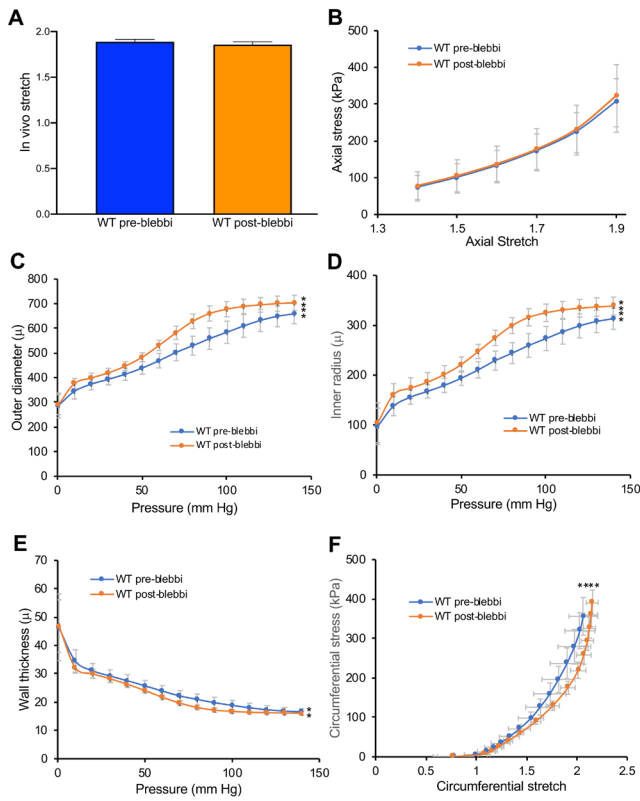
Figure 1

Reduced smooth muscle contraction with blebbistatin selectively affects circumferential arterial mechanics in WT carotid arteries. Right carotid arteries isolated from male WT (C57BL/6J) mice (n = 6) were analyzed by pressure myography and then immediately reanalyzed after treatment with blebbistatin (see Methods). (A) In vitro stretch as determined from axial force-length tests. (B) Axial stress–stretch curves obtained at 100 mmHg. (C) Changes in outer diameter with increasing pressure. (D and E) Changes in vessel inner radius and wall thickness, respectively, with pressure. (F) Circumferential stress–stretch curves with data points showing results at 0–140 mmHg in increments of 10 mm. Statistical significance was determined by two-tailed t-test (panel A) or two-way ANOVA (panels B-F). In F, the indicated statistical significance was the same for both stretch and stress. The axial stress–stretch curves shown in panel B and in Supplementary Fig. 1A, B and C were taken from the same mice and biomechanical testing but at different pressures.

Figure 2

Effect of EGTA on passive arterial mechanics in WT carotid arteries. Right carotid arteries isolated from male WT (C57BL/6J) mice (n = 5) were analyzed by pressure myography and then immediately reanalyzed after treatment with 2 mM EGTA. (A) In vitro stretch as determined from axial force-length tests. (B) Axial stress–stretch curve obtained at 100 mmHg. (C, D and E) Changes in vessel outer diameter, inner radius, and wall thickness, respectively, with pressure. (F) Circumferential stress–stretch curves with data points showing results at 0–140 mmHg in increments of 10 mm. Statistical significance was determined by two-tailed t-test (panel A) or two-way ANOVA (panels B-F). In F, the indicated statistical significance was the same for both stretch and stress. The axial stress–stretch curves shown in panel B and in Supplementary Fig. 1D, E and F were taken from the same mice and biomechanical testing but at different pressures.

to pressure. These effects were associated with reduced circumferential stiffness as shown by the overall right shift in the stress–stretch curve (Fig. 1F). We noted, however, an increase in the slope of the stress–stretch curve for blebbistatin-treated arteries at circumferential stretches >2.

As calcium is critical to SMC contractility (34, 35), we tested the requirement for calcium by performing the entire set of passive testing of WT carotid arteries in the absence vs presence of the calcium chelator, EGTA (Fig. 2). The effects of EGTA were very similar to those seen in blebbistatin, with the primary effect being on circumferential (Fig. 2F) rather than axial arterial stiffness (Fig. 2B). We note, however, that EGTA did reduce axial stiffness at 80 mm Hg (but
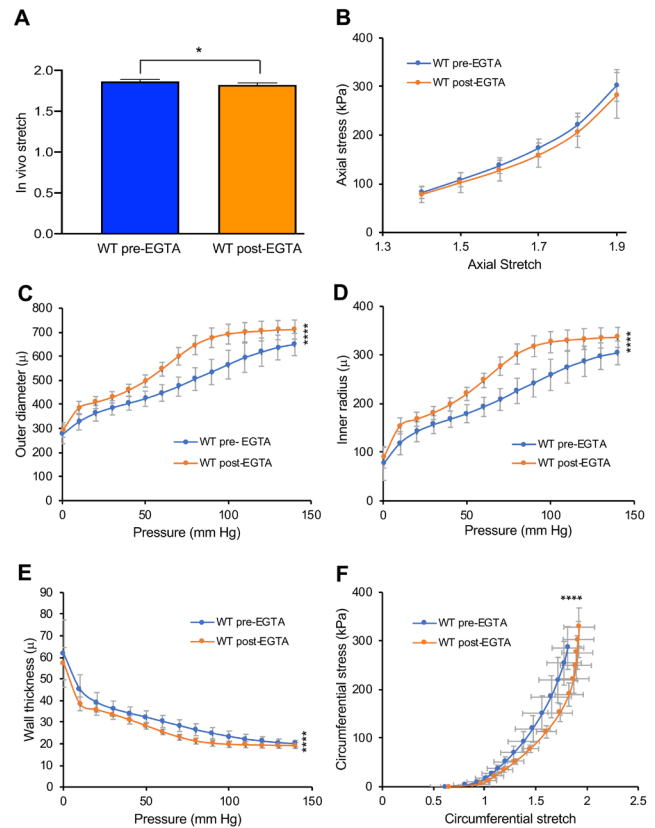
not 100, 120, or 140 mm Hg; Figs 2B and Supplementary Fig. 1D, E, F). The basis for this isolated effect is not clear but may relate to the fact that calcium chelation with EGTA can also disrupt cell–cell adhesion through cadherins and cell–ECM adhesion through certain integrins (36, 37, 38, 39).

Smooth muscle-specific deletion of FAK affects vessel wall thickness and reduces circumferential arterial stiffness

Our finding that cell contraction contributes to arterial geometry and circumferential arterial stiffness led us

to postulate that upstream regulators of contractility should play a role in this effect. We were particularly interested in exploring the role of FAK because it is a canonical mechanosensor that transduces signals from multiple ECM–integrins complexes, because its activating phosphorylation in SMCs is stimulated by ECM stiffness (31, 32) and because it has been reported to promote smooth muscle cell contractility and phenylephrine-induced arterial stiffening (26, 40, 41).

We generated floxed FAK mice harboring a SMC-specific, tamoxifen-inducible Cre transgene (FAKᶠᶠ;iCre mice), treated the mice with vehicle (ethanol) or tamoxifen, and studied the role of SMC FAK on arterial biology. FAK expression was strongly expressed in the carotid medial layer of mice treated with vehicle and strongly reduced in the tamoxifen-treated mice (Fig. 3A and B). In contrast and as expected from the high specificity of the Cre transgene (30), adventitial FAK abundance was not significantly affected by tamoxifen (Fig. 3A and B). Carotid artery morphology, as determined by H&E staining, appeared normal in both the vehicle- and tamoxifen-treated mice (Fig. 3A).

We then performed biaxial inflation-extension tests to assess the effects of FAK deletion on arterial mechanics. Like the blebbistatin or EGTA treatments, axial arterial mechanics, as determined by the IVS and axial stress–stretch relationship, were not affected by the deletion of SMC FAK (Fig. 4A, B and Supplementary Fig. 1G, H, I). Somewhat unexpectedly, the outer diameter (Fig. 3C) and inner radius (Fig. 4D) responses to pressure were also not affected by the deletion of SMC FAK. However, wall thickness was reduced by the deletion of SMC FAK (Fig. 4E), as was circumferential arterial stiffness as determined by the right-shift in the stress–stretch curves (Fig. 4F). Thus, deletion of SMC FAK recapitulated some but not all of the circumferential effects seen with blebbistatin or EGTA.

Reduced circumferential arterial stiffness in FAK-deficient mice occurs without changes in fibrillar collagens or smooth muscle differentiation markers

Because Cre-mediated excision of FAK occurred over 2–3 weeks (see Methods), we considered the possibility that the reduced circumferential stiffness of FAK-deficient carotid arteries might reflect remodeling of the arterial ECM, and particularly a change in the abundance of fibrillar collagens or integrity of elastin, the ECM components most commonly considered to regulate ECM mechanics. However, the abundance of all three arterial fibrillar collagens (I, III, and
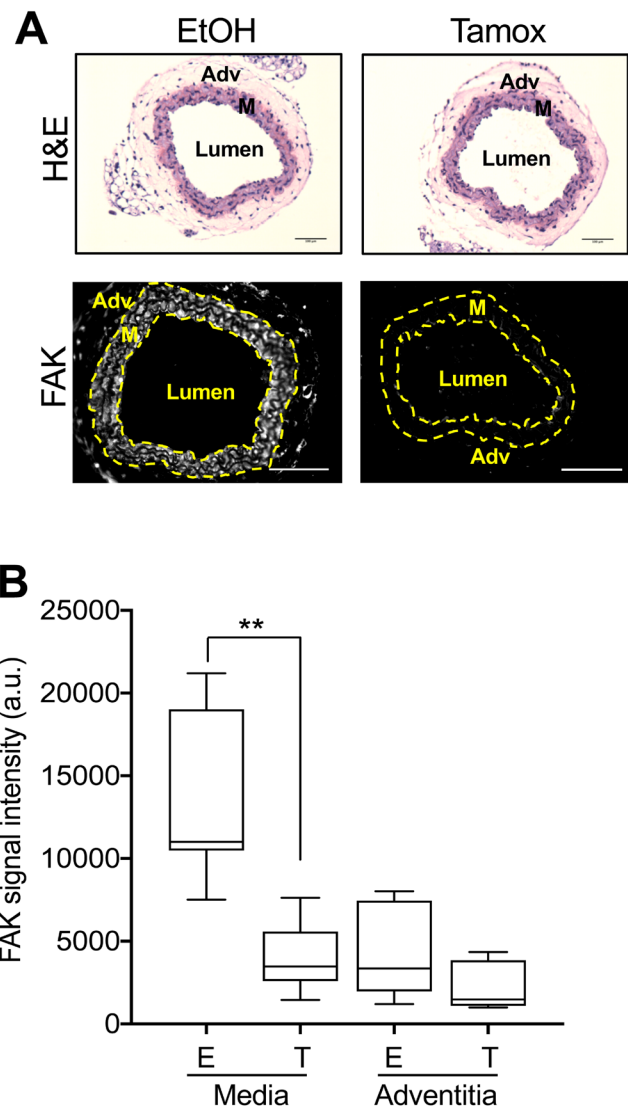
Figure 3

Deletion of SMC FAK. (A) Images of carotid artery cross-sections from FAKᶠ/ᶠ;iCre mice that had been treated with vehicle (ethanol) or tamoxifen and stained with H&E and an antibody to FAK. Scale bars = 100 μm. Dashed lines in panel A approximate the positions of the external and internal elastic laminae, which separate the medial (M) and adventitial (Adv) layers. (B) The immunostaining results in A were quantified and graphed as box plots with Tukey whiskers; *n* = 6–7. Statistical significance was determined by two-tailed Mann–Whitney tests comparing ethanol to tamoxifen within the media and adventitia.

V) as well as their expected preferential localizations to the adventitia (collagen-I) or media (collagen-III and -V) were similar in the vehicle- and tamoxifen-treated carotid arteries (Fig. 5A and B). Elastin integrity was also unaffected by tamoxifen treatment (Supplementary Fig. 2).

We also considered the possibility that FAK deletion might promote the transition of arterial smooth muscle
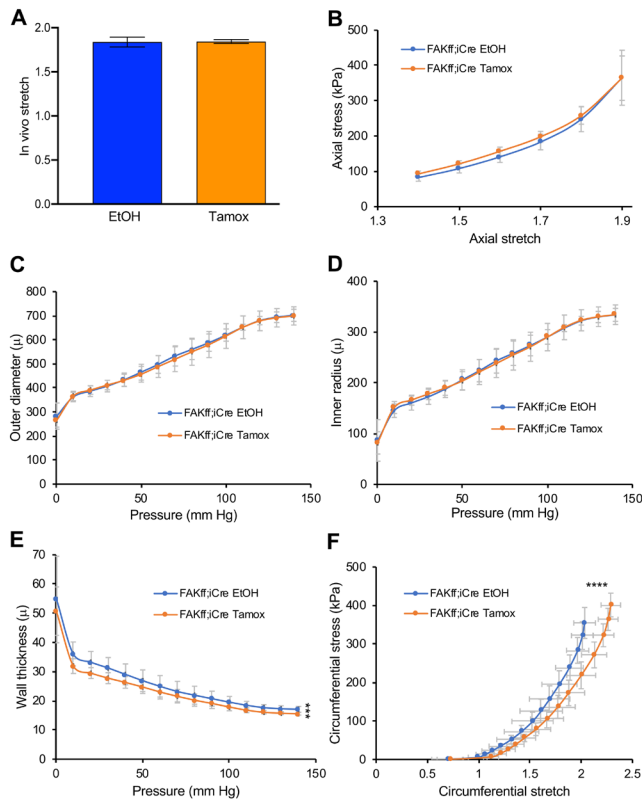
Figure 4

Deletion of SMC FAK attenuates circumferential arterial stiffness. Freshly isolated right carotid arteries from FAK^{ff}-iCre mice were treated with ethanol (EtOH) or tamoxifen (Tamox) and analyzed by pressure myography (n = 5 per condition). (A) In vitro stretch as determined from axial force-length tests. (B) Axial stress–stretch curves obtained at 100 mmHg. (C) Changes in outer diameter with increasing pressure. (D and E) Changes in vessel inner radius and wall thickness, respectively, with pressure. (F) Circumferential stress–stretch curves with data points showing results at 0–140 mmHg in increments of 10 mm. Statistical significance was determined by two-tailed t-test (panel A) or two-way ANOVA (panels B-F). In F, the indicated statistical significance was the same for both stretch and stress. The axial stress–stretch curves shown in panel B and in Supplementary Fig. 1G, H and I were taken from the same mice and biomechanical testing but at different pressures.

Figure 5

Arterial fibrillar collagens abundance is not affected by deletion of SMC FAK. (A) Images of carotid artery cross-sections from FAK$^{f/f}$;iCre mice that had been treated with vehicle (ethanol) or tamoxifen and stained with antibodies to collagen-I, collagen-III, or collagen-V. Scale bars = 100 μm. Dashed lines approximate the positions of the external and internal elastic laminae, which separate the medial (M) and adventitial (Adv) layers. (B) The immunostaining results in A were quantified and graphed as box plots with Tukey whiskers; *n* = 5–7. Statistically significant differences were not detected when comparing (by two-tailed Mann–Whitney tests) ethanol vs tamoxifen treatment within each tissue layer.

cells toward a de-differentiated phenotype. However, the expression of SM-MHC and SMA proteins, two well-established markers of the contractile smooth muscle phenotype (see Introduction), was similar in the carotid arteries of the vehicle- and tamoxifen-treated mice (Fig. 6A and B). As de-differentiated SMCs are thought to be responsible for ECM remodeling, the lack of a notable FAK effect on SMC differentiation supports and extends our results with the arterial collagens. Collectively, these results argue that the reduced circumferential arterial stiffness we observe upon deletion of SMC FAK is not due to a remodeled ECM arising from an altered SMC differentiation phenotype.
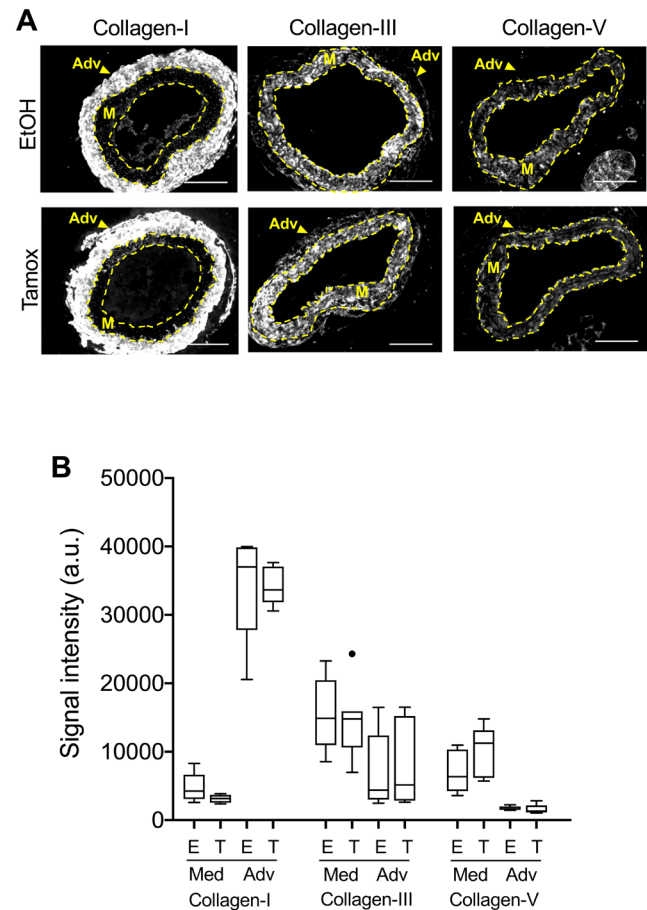
Acute inhibition of cell contractility attenuates the effect of FAK deletion on wall thickness and circumferential arterial stiffness

Given that FAK depletion from SMCs did not strongly affect SMC differentiation markers or the arterial collagens and elastin, we tested whether deletion of SMC FAK reduced arterial contractility. Consistent with results by others (26, 40, 41), we found that arterial contraction to KCl was reduced in the carotid arteries lacking SMC FAK (Fig. 7). We then eliminated smooth muscle contraction as a possible FAK target by exposing the vehicle- and tamoxifen-treated carotids from FAK^{ff};iCre mice to blebbistatin and asked if the presence or absence of SMC FAK would still affect
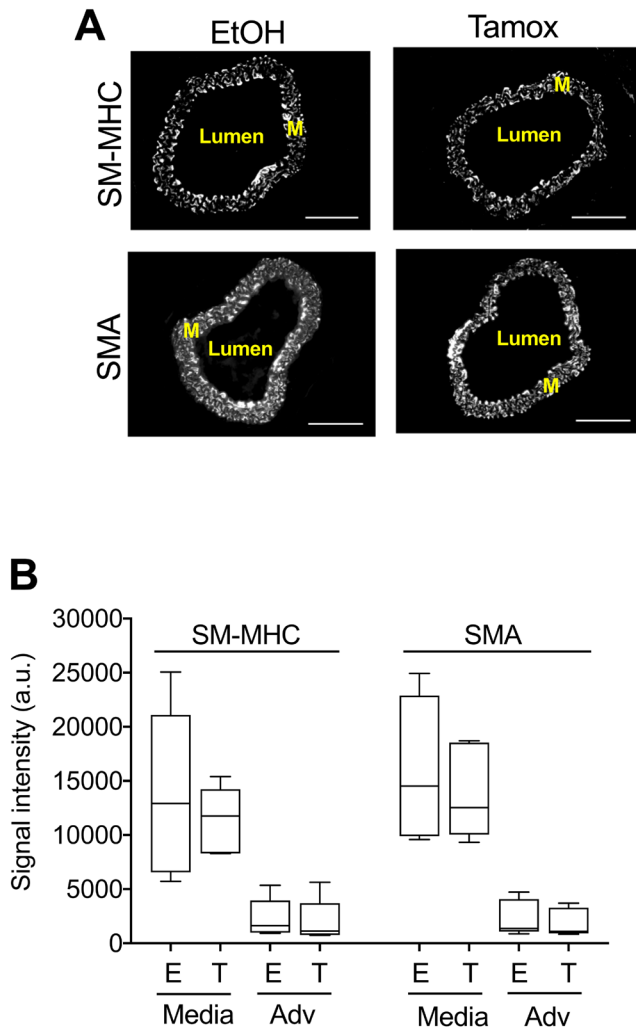
Figure 6

Similar expression of SMC differentiation markers upon deletion of SMC FAK. (A) Images of carotid artery cross-sections from FAK$^{f/f}$;iCre mice that had been treated with vehicle (ethanol) or tamoxifen and immunostained with antibodies to SM-MHC or SMA show medial (M) localization of the two contractile markers. Scale bars = 100 μm. (B) Immunostaining results in A were quantified and graphed as box plots with Tukey whiskers; $n = 7$. Statistically significant differences were not detected when comparing (by two-tailed Mann–Whitney tests) ethanol vs tamoxifen treatment within the media and adventitia (Adv).

Figure 7

Deletion of SMC FAK reduces carotid arterial contraction. FAK^{ff}-iCre mice were treated with ethanol or tamoxifen. Freshly isolated left carotid arteries were mounted on the pressure myograph and submerged in HBSS. Mounted vessels were preconditioned by stretching them axially to 1.15 times their UVL at 40 mmHg for 15 min and then 1.3 times their UVL at 60 mmHg for 15 min. The preconditioned vessels were brought to their IVS and pressurized to 100 mmHg. Increasing concentrations of KCl (10^{-4} M to 10^{-1} M in HBSS; 5 mL) were added to the vessel chamber sequentially at 10-min intervals or once the constriction plateau had been reached. Each new KCl solution was added after removing the prior KCl solution, and the extent of contraction to each KCl solution (defined as the change in outer diameter relative to baseline) was measured when the vessel's outer diameter had reached its plateau (~5 min after each treatment). The baseline (dashed line) was defined as the contraction seen with 10^{-4} M KCl (this concentration approximated the KCl concentration in HBSS) and set to zero. Data were passed through a Grubb's test and then analyzed for statistical significance by one-way ANOVA; $n = 6$ for ethanol and $n = 7$–8 for tamoxifen-treated arteries.

arterial mechanics. We used blebbistatin in this analysis rather than EGTA to avoid potential confounding effects of disrupted cell–cell and/or cell–ECM adhesion.

The presence or absence of SMC FAK did not significantly affect axial mechanics in the blebbistatin-treated arteries as determined by the IVS or axial stress–stretch relationship (Fig. 8A, B and Supplementary Fig. 1J, K, L). Similarly, the outer diameter and inner radius responses to increasing pressure in the blebbistatin-treated arteries remained unaffected by the presence or absence of SMC FAK (Fig. 8C and D). However, blebbistatin treatment eliminated
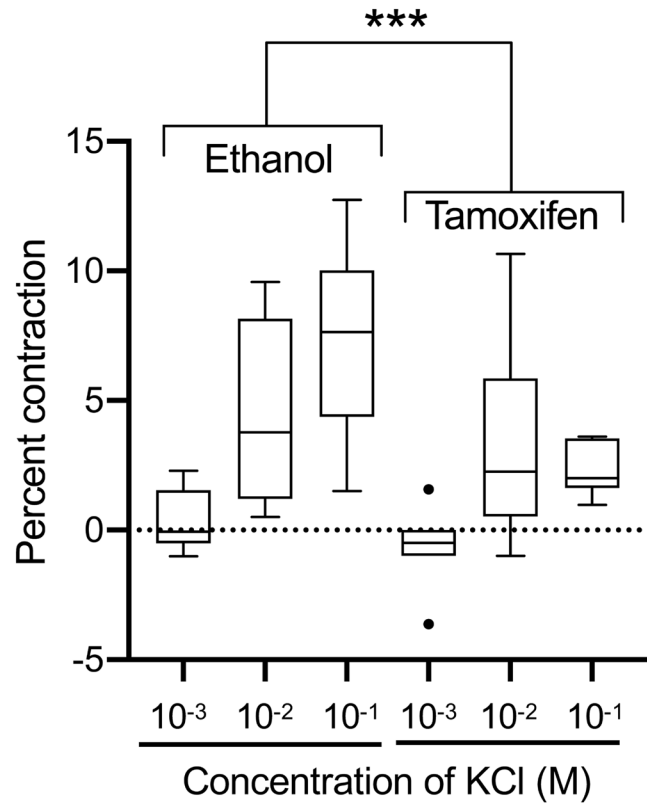
the ability of FAK to regulate wall thickness in response to pressure (Fig. 8E), and this effect was associated with near complete loss of the FAK effect on circumferential arterial stiffness (Fig. 8F). These results causally link the effects of FAK on smooth muscle contractility to the FAK effects on arterial geometry and stiffness. Note that the outer diameter, inner radius, wall thickness, and circumferential stress–stretch relationship in the carotids of these conditional FAK mice remained sensitive to blebbistatin (Supplementary Fig. 3), much like that seen in the WT vessels.
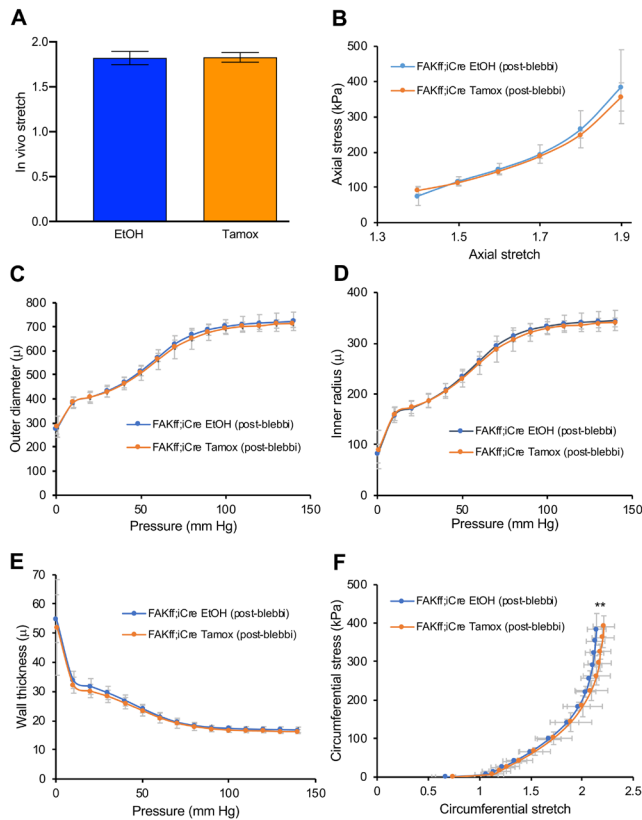
Figure 8

Blebbistatin eliminates the effect of SMC FAK deletion on arterial wall thickness and circumferential stiffness. Each carotid artery tested in Fig. 4 was immediately treated with blebbistatin and reanalyzed. (A) In vitro stretch as determined from axial force-length tests. (B) Axial stress–stretch curves obtained at 100 mmHg. (C) Changes in outer diameter with increasing pressure. (D-E) Changes in vessel inner radius and wall thickness, respectively, with pressure. (F) Circumferential stress–stretch curves with data points showing results at 0–140 mmHg in increments of 10 mm. Statistical significance was determined as in Fig. 4. In F, statistical significance is shown for stretch; differences in stress were not significant. The axial stress–stretch curves shown in panel B and in Supplementary Fig. 1J, K and L were taken from the same mice and biomechanical testing but at different pressures.

Finally, we repeated the entire panel of passive mechanical testing on FAK-containing and FAK-deficient arteries treated with the MLCK, ML7 (Supplementary Fig. 4). Consistent with the results above, deletion of SMC FAK did not affect the metrics of axial stiffness (Supplementary Fig. 4A, B, C, D and E; compare EtOH vs Tamox solid lines), but it reduced arterial wall thickness (Supplementary Fig. 4H; compare EtOH vs Tamox solid lines) and circumferential stiffness (Supplementary Fig. 4I; EtOH vs Tamox solid lines). As with blebbistatin, the effects of SMC FAK deletion were lost when the arteries were treated with ML7 (Supplementary Fig. 4H and I; EtOH vs Tamox dashed lines).

Discussion

The work presented here examines the direct role of SMCs and cellular contraction in large artery stiffness. Prior work in this area has provided provocative results (see Introduction) but has not incorporated the role of arterial pressure, interrogated possible anisotropic effects of cell contractility, or identified molecular regulators genetically. Our work addresses these limitations, and our findings indicate that (i) contractility plays a clear role in the large artery stiffness response to pressure, (ii) SMC FAK contributes to this effect, and (iii) the consequence of cell contractility and SMC FAK on arterial stiffness is anisotropic (circumferential) and due to changes in vessel geometry. FAK deletion did not phenocopy all the geometric effects seen upon inhibition of cell contractility with blebbistatin or EGTA, but the reductions in wall thickness seen with reduced contractility (whether through drug treatment or FAK deletion) were very similar. We have previously described a direct relationship between traction force and cell area in SMCs (42), suggesting that the reductions in SMC contractility and arterial wall thickness observed in this report may be related.

While the blebbistatin, EGTA, and ML7 effects on arterial geometry and circumferential stiffness were rapid, the conditional deletion of SMC FAK occurred over 2–3 weeks. The protracted nature of this genetic deletion raised an alternative possibility that the observed FAK effect on wall thickness and the circumferential stress–stretch relationship might reflect a change in SMC differentiation rather than a direct effect on SMC contractility. However, the expression levels of SM-MHC and SMA, the two best-studied SMC differentiation markers, were not affected by FAK deletion. Moreover, ECM synthesis is much more pronounced in de-differentiated (synthetic) vs differentiated (contractile) SMCs, but we found similar fibrillar collagen levels in FAK-expressing and FAK-deleted carotid arteries under the condition of our analysis. Finally, the effect of FAK deletion on vessel wall thickness and the circumferential stress–stretch relationship was lost when contractility was blocked by acute blebbistatin treatment.

In prior work using cells cultured on deformable substrata and *in vivo* vascular injury, we identified a stiffness-stimulated signaling module that is comprised of FAK, Src, and p130Cas and leads to the stiffness-dependent activation of Rac (31, 32). It is now interesting to view this prior work in the context of studies from Morgan and colleagues who reported activating phosphorylations of FAK and Cas during phenylephrine-induced arterial stiffening (26, 27). Both sets of studies indicate that the

FAK-Src-Cas signaling module is stiffness-regulated and also describe a requirement for actomyosin contraction to maintain this signaling module in an active state. We therefore speculate that Rac activity may be upregulated in stiffened arteries, and it might be interesting to look for changes in Rac effectors in stretched aortic rings or pressure-induced extension of carotid arteries.

The Rho/Rho kinase pathway is an established regulator of SMC contractility (see Introduction), and Rho signaling is activated by both cadherin-mediated cell–cell adhesion and integrin-mediated cell–ECM adhesion (43). Our current experiments using EGTA, blebbistatin, ML7, and SMC FAK deficiency cannot resolve the relative contributions of different upstream contractility regulators and pathways to arterial stiffness. We have started to investigate this issue by generating and testing mice conditionally deficient for SMC N-cadherin, and we suggest that a similar conditional knock-out approach of putative contractility regulators (rather than the use of systemic pharmacologic reagents) will be increasingly important in future studies as it allows for selective targeting of medial SMCs, intimal endothelial cells, and adventitial fibroblasts.

We note that blebbistatin, EGTA, ML7, and SMC FAK deletion do not have identical effects on circumferential arterial responses to pressure. For example, all the treatments reduced wall thickness, but SMC FAK deletion did not alter the inner radius response to pressure. Thus, the inner radius response to pressure is independent of SMC FAK. One possible explanation for this data is that a different SMC focal adhesion mechanosensor regulates the inner radius response that is seen upon pharmacologic inhibition of contractility. Alternatively, the different effects of blebbistatin, EGTA, and ML7 vs SMC FAK deficiency on vessel geometry may reflect a systemic effect of the drugs on adventitial fibroblast or intimal endothelial myosin-II as compared to the tissue-specific effect of SMC FAK deletion. We also note that blebbistatin, EGTA, and ML7 (but not SMC FAK deletion) reduced axial stiffness to varying degrees at 80 mmHg but not at 100, 120, or 140 mmHg. This limited axial effect might also reflect systemic effects of the drugs on vessel endothelial cells and/or fibroblasts. Finally, we note that the effects of ML7 on vessel outer diameter, inner radius, and circumferential stiffness were less pronounced than those seen with blebbistatin or EGTA. Perhaps, this difference relates to different efficiencies of drug uptake into the carotid artery or different efficiencies of contraction inhibition. Additional tissue-specific knock-outs as discussed above would help to resolve these possibilities.

Our results reveal an anisotropic effect of cell contractility and SMC FAK on circumferential arterial stiffness, and it is tempting to speculate on how this might occur. One possibility relates to the fact that SMCs (2, 44) and their actin stress fibers (44) are mostly oriented circumferentially within the arterial medial layer. Since FAK is contained within the focal adhesions that anchor these circumferentially oriented stress fibers, reduced SMC contractility upon FAK deletion might target circumferential mechanics more than axial. Unraveling how SMC contractility, FAK, and other focal adhesion proteins might cooperate with ECM remodeling/integrin signaling and cell–cell adhesion to determine directionally selective arterial stiffening is likely to provide valuable insight into the dynamic changes in arterial mechanics that occur with vascular development, age, and disease.

Declaration of interest
The authors declare that there is no conflict of interest that could be perceived as prejudicing the impartiality of the research reported.

Author contribution statement
Experiments were designed by R K A and performed by E R and T X. E R, T X, and R K A analyzed data. R K A and E R prepared the manuscript text and figures.

References

1 Shirwany NA & Zou MH. Arterial stiffness: a brief review. *Acta Pharmacologica Sinica* 2010 **31** 1267–1276. (https://doi.org/10.1038/aps.2010.123)

2 Kohn JC, Lampi MC & Reinhart-King CA. Age-related vascular stiffening: causes and consequences. *Frontiers in Genetics* 2015 **6** 112. (https://doi.org/10.3389/fgene.2015.00112)

3 Saphirstein RJ & Morgan KG. The contribution of vascular smooth muscle to aortic stiffness Across length scales. *Microcirculation* 2014 **21** 201–207. (https://doi.org/10.1111/micc.12101)

4 Majesky MW, Dong XR, Hoglund V, Mahoney WM & Daum G. The adventitia: a dynamic interface containing resident progenitor cells. *Arteriosclerosis, Thrombosis, and Vascular Biology* 2011 **31** 1530–1539. (https://doi.org/10.1161/ATVBAHA.110.221549)

5 Ferruzzi J, Bersi MR & Humphrey JD. Biomechanical phenotyping of central arteries in health and disease: advantages of and methods for murine models. *Annals of Biomedical Engineering* 2013 **41** 1311–1330. (https://doi.org/10.1007/s10439-013-0799-1)

6 Wagenseil JE & Mecham RP. Vascular extracellular matrix and arterial mechanics. *Physiological Reviews* 2009 **89** 957–989. (https://doi.org/10.1152/physrev.00041.2008)

7 Brankovic SA, Hawthorne EA, Yu X, Zhang Y & Assoian RK. MMP12 deletion preferentially attenuates axial stiffening of aging arteries. *Journal of Biomechanical Engineering* 2019 **141** 0810041–0810049. (https://doi.org/10.1115/1.4043322)

8 von Kleeck R, Roberts E, Castagnino P, Bruun K, Brankovic SA, Hawthorne EA, Xu T, Tobias JW & Assoian RK. Arterial stiffness and cardiac dysfunction in Hutchinson–Gilford progeria syndrome corrected by inhibition of lysyl oxidase. *Life Science Alliance* 2021 **4** e202000997. (https://doi.org/10.26508/lsa.202000997)

9 Gaballa MA, Jacob CT, Raya TE, Liu J, Simon B & Goldman S. Large artery remodeling during aging: biaxial passive and active stiffness. *Hypertension* 1998 **32** 437–443. (https://doi.org/10.1161/01.hyp.32.3.437)

10 Diaz-Otero JM, Garver H, Fink GD, Jackson WF & Dorrance AM. Aging is associated with changes to the biomechanical properties of the posterior cerebral artery and parenchymal arterioles. *American Journal of Physiology: Heart and Circulatory Physiology* 2016 **310** H365–H375. (https://doi.org/10.1152/ajpheart.00562.2015)

11 Ferruzzi J, Bersi MR, Mecham RP, Ramirez F, Yanagisawa H, Tellides G & Humphrey JD. Loss of elastic fiber integrity compromises common carotid artery function: implications for vascular aging. *Artery Research* 2016 **14** 41–52. (https://doi.org/10.1016/j.artres.2016.04.001)

12 Thyberg J, Hedin U, Sjolund M, Palmberg L & Bottger BA. Regulation of differentiated properties and proliferation of arterial smooth muscle cells. *Arteriosclerosis* 1990 **10** 966–990. (https://doi.org/10.1161/01.atv.10.6.966)

13 Yoshida T & Owens GK. Molecular determinants of vascular smooth muscle cell diversity. *Circulation Research* 2005 **96** 280–291. (https://doi.org/10.1161/01.RES.0000155951.62152.2e)

14 Owens GK. Regulation of differentiation of vascular smooth muscle cells. *Physiological Reviews* 1995 **75** 487–517. (https://doi.org/10.1152/physrev.1995.75.3.487)

15 Wang Z, Wang DZ, Pipes GCT & Olson EN. Myocardin is a master regulator of smooth muscle gene expression. *PNAS* 2003 **100** 7129–7134. (https://doi.org/10.1073/pnas.1232341100)

16 Olson EN & Nordheim A. Linking actin dynamics and gene transcription to drive cellular motile functions. *Nature Reviews: Molecular Cell Biology* 2010 **11** 353–365. (https://doi.org/10.1038/nrm2890)

17 Klein EA, Yin L, Kothapalli D, Castagnino P, Byfield FJ, Xu T, Levental I, Hawthorne E, Janmey PA & Assoian RK. Cell-cycle control by physiological matrix elasticity and in vivo tissue stiffening. *Current Biology* 2009 **19** 1511–1518. (https://doi.org/10.1016/j.cub.2009.07.069)

18 Kothapalli D, Liu SL, Bae YH, Monslow J, Xu T, Hawthorne EA, Byfield FJ, Castagnino P, Rao S, Rader DJ, *et al.* Cardiovascular protection by ApoE and ApoE-HDL linked to suppression of ECM gene expression and arterial stiffening. *Cell Reports* 2012 **2** 1259–1271. (https://doi.org/10.1016/j.celrep.2012.09.018)

19 Liu SL, Bae YH, Yu C, Monslow J, Hawthorne EA, Castagnino P, Branchetti E, Ferrari G, Damrauer SM, Puré E, *et al.* Matrix metalloproteinase-12 is an essential mediator of acute and chronic arterial stiffening. *Scientific Reports* 2015 **5** 17189. (https://doi.org/10.1038/srep17189)

20 Gao YZ, Saphirstein RJ, Yamin R, Suki B & Morgan KG. Aging impairs smooth muscle-mediated regulation of aortic stiffness: a defect in shock absorption function? *American Journal of Physiology: Heart and Circulatory Physiology* 2014 **307** H1252–H1261. (https://doi.org/10.1152/ajpheart.00392.2014)

21 Qiu H, Zhu Y, Sun Z, Trzeciakowski JP, Gansner M, Depre C, Resuello RR, Natividad FF, Hunter WC, Genin GM, *et al.* Short communication: vascular smooth muscle cell stiffness as a mechanism for increased aortic stiffness with aging. *Circulation Research* 2010 **107** 615–619. (https://doi.org/10.1161/CIRCRESAHA.110.221846)

22 Sehgel NL, Sun Z, Hong Z, Hunter WC, Hill MA, Vatner DE, Vatner SF & Meininger GA. Augmented vascular smooth muscle cell stiffness and adhesion when hypertension is superimposed on aging. *Hypertension* 2015 **65** 370–377. (https://doi.org/10.1161/HYPERTENSIONAHA.114.04456)

23 Sehgel NL, Zhu Y, Sun Z, Trzeciakowski JP, Hong Z, Hunter WC, Vatner DE, Meininger GA & Vatner SF. Increased vascular smooth muscle cell stiffness: a novel mechanism for aortic stiffness in hypertension. *American Journal of Physiology: Heart and Circulatory Physiology* 2013 **305** H1281–H1287. (https://doi.org/10.1152/ajpheart.00232.2013)

24 Zhou N, Lee JJ, Stoll S, Ma B, Costa KD & Qiu H. Rho kinase regulates aortic vascular smooth muscle cell stiffness via actin/SRF/myocardin in hypertension. *Cellular Physiology and Biochemistry* 2017 **44** 701–715. (https://doi.org/10.1159/000485284)

25 Van Aelst L & D'Souza-Schorey C. Rho GTPases and signaling networks. *Genes and Development* 1997 **11** 2295–2322. (https://doi.org/10.1101/gad.11.18.2295)

26 Saphirstein RJ, Gao YZ, Jensen MH, Gallant CM, Vetterkind S, Moore JR & Morgan KG. The focal adhesion: a regulated component of aortic stiffness. *PLoS ONE* 2013 **8** e62461. (https://doi.org/10.1371/journal.pone.0062461)

27 Singh K, Kim AB & Morgan KG. Non-muscle myosin II regulates aortic stiffness through effects on specific focal adhesion proteins and the non-muscle cortical cytoskeleton. *Journal of Cellular and Molecular Medicine* 2021 **25** 2471–2483. (https://doi.org/10.1111/jcmm.16170)

28 Korneva A & Humphrey JD. Maladaptive aortic remodeling in hypertension associates with dysfunctional smooth muscle contractility. *American Journal of Physiology: Heart and Circulatory Physiology* 2019 **316** H265–H278. (https://doi.org/10.1152/ajpheart.00503.2017)

29 Eberth JF & Humphrey JD. Reduced smooth muscle contractile capacity facilitates maladaptive arterial remodeling. *Journal of Biomechanical Engineering* 2022 **144** 044503. (https://doi.org/10.1115/1.4052888)

30 Wirth A, Benyo Z, Lukasova M, Leutgeb B, Wettschureck N, Gorbey S, Orsy P, Horváth B, Maser-Gluth C, Greiner E, *et al.* G12-G13-LARG-mediated signaling in vascular smooth muscle is required for salt-induced hypertension. *Nature Medicine* 2008 **14** 64–68. (https://doi.org/10.1038/nm1666)

31 Mui KL, Bae YH, Gao L, Liu SL, Xu T, Radice GL, Chen CS & Assoian RK. N-cadherin induction by ECM stiffness and FAK overrides the spreading requirement for proliferation of vascular smooth muscle cells. *Cell Reports* 2015 **10** 1477–1486. (https://doi.org/10.1016/j.celrep.2015.02.023)

32 Bae YH, Mui KL, Hsu BY, Liu SL, Cretu A, Razinia Z, Xu T, Puré E & Assoian RK. A FAK-Cas-Rac-lamellipodin signaling module transduces extracellular matrix stiffness into mechanosensitive cell cycling. *Science Signaling* 2014 **7** ra57. (https://doi.org/10.1126/scisignal.2004838)

33 von Kleeck R, Castagnino P, Roberts E, Talwar S, Ferrari G & Assoian RK. Decreased vascular smooth muscle contractility in Hutchinson–Gilford progeria syndrome linked to defective smooth muscle myosin heavy chain expression. *Scientific Reports* 2021 **11** 10625. (https://doi.org/10.1038/s41598-021-90119-4)

34 Adelstein RS & Sellers JR. Effects of calcium on vascular smooth muscle contraction. *American Journal of Cardiology* 1987 **59** 4B–10B. (https://doi.org/10.1016/0002-9149(87)90076-2)

35 Walsh MP. Calmodulin and the regulation of smooth muscle contraction. *Molecular and Cellular Biochemistry* 1994 **135** 21–41. (https://doi.org/10.1007/BF00925958)

36 Brown KL, Banerjee S, Feigley A, Abe H, Blackwell TS, Pozzi A, Hudson BG & Zent R. Salt-bridge modulates differential calcium-mediated ligand binding to integrin α1- and α2-I domains. *Scientific Reports* 2018 **8** 2916. (https://doi.org/10.1038/s41598-018-21231-1)

37 Zhang K & Chen J. The regulation of integrin function by divalent cations. *Cell Adhesion and Migration* 2012 **6** 20–29. (https://doi.org/10.4161/cam.18702)

38 Nagar B, Overduin M, Ikura M & Rini JM. Structural basis of calcium-induced E-cadherin rigidification and dimerization. *Nature* 1996 **380** 360–364. (https://doi.org/10.1038/380360a0)

39 Tamura K, Shan WS, Hendrickson WA, Colman DR & Shapiro L. Structure-function analysis of cell adhesion by neural (N-) cadherin. *Neuron* 1998 **20** 1153–1163. (https://doi.org/10.1016/s0896-6273(00)80496-1)

40 Xie Y, Han KH, Grainger N, Li W, Corrigan RD & Perrino BA. A role for focal adhesion kinase in facilitating the contractile responses of murine gastric fundus smooth muscles. *Journal of Physiology* 2018 **596** 2131–2146. (https://doi.org/10.1113/JP275406)

41 Tang DD & Gunst SJ. Depletion of focal adhesion kinase by antisense depresses contractile activation of smooth muscle. *American Journal of Physiology: Cell Physiology* 2001 **280** C874–C883. (https://doi.org/10.1152/ajpcell.2001.280.4.C874)

42 Talwar S, Kant A, Xu T, Shenoy VB & Assoian RK. Mechanosensitive smooth muscle cell phenotypic plasticity emerging from a null state and the balance between Rac and Rho. *Cell Reports* 2021 **35** 109019. (https://doi.org/10.1016/j.celrep.2021.109019)

43 Mui KL, Chen CS & Assoian RK. The mechanical regulation of integrin-cadherin crosstalk organizes cells, signaling and forces. *Journal of Cell Science* 2016 **129** 1093–1100. (https://doi.org/10.1242/jcs.183699)

44 Liu SQ. Influence of tensile strain on smooth muscle cell orientation in rat blood vessels. *Journal of Biomechanical Engineering* 1998 **120** 313–320. (https://doi.org/10.1115/1.2797996)